Reversal of microRNA-150 silencing disadvantages crizotinib-resistant NPM-ALK(+) cell growth

Coralie Hoareau-Aveilla,[1,2,3] Thibaud Valentin,[1,2,3] Camille Daugrois,[1,2,3] Cathy Quelen,[1,2,3] Géraldine Mitou,[1,2,3] Samuel Quentin,[4] Jinsong Jia,[5] Salvatore Spicuglia,[5] Pierre Ferrier,[5] Monica Ceccon,[6,7] Sylvie Giuriato,[1,2,3,7] Carlo Gambacorti-Passerini,[6,7] Pierre Brousset,[1,2,3,7,8,9] Laurence Lamant,[1,2,3,7,8,9] and Fabienne Meggetto[1,2,3,7,8,9]

[1]Inserm, UMR1037 Cancer Research Center of Toulouse (CRCT), Toulouse, France. [2]Université Toulouse III-Paul Sabatier, UMR1037 CRCT, Toulouse, France. [3]CNRS, ERL5294 CRCT, Toulouse, France. [4]Hematology Laboratory, Hospital Saint-Louis, Paris, France. [5]Centre d'Immunologie de Marseille-Luminy, Aix Marseille Université UM2, Inserm, U1104, CNRS UMR7280, Marseille, France. [6]Department of Health Sciences, University of Milano-Bicocca, Monza, Italy. [7]European Research Initiative on ALK-Related Malignancies (ERIA). [8]Institut Carnot Lymphome-CALYM, Toulouse, France. [9]Laboratoire d'Excellence Toulouse Cancer-TOUCAN, Toulouse, France.

The regulatory microRNA miR-150 is involved in the development of hemopathies and is downregulated in T-lymphomas, such as anaplastic large-cell lymphoma (ALCL) tumors. ALCL is defined by the presence or absence of translocations that activate the anaplastic lymphoma kinase (ALK), with nucleophosmin-ALK (NPM-ALK) fusions being the most common. Here, we compared samples of primary NPM-ALK(+) and NPM-ALK(–) ALCL to investigate the role of miR-150 downstream of NPM-ALK. Methylation of the *MIR150* gene was substantially elevated in NPM-ALK(+) biopsies and correlated with reduced miR-150 expression. In NPM-ALK(+) cell lines, DNA hypermethylation–mediated miR-150 repression required ALK-dependent pathways, as ALK inhibition restored miR-150 expression. Moreover, epigenetic silencing of miR-150 was due to the activation of STAT3, a major downstream substrate of NPM-ALK, in cooperation with DNA methyltransferase 1 (DNMT1). Accordingly, miR-150 repression was turned off following treatment with the DNMT inhibitor, decitabine. In murine NPM-ALK(+) xenograft models, miR-150 upregulation induced antineoplastic activity. Treatment of crizotinib-resistant NPM-ALK(+) KARPAS-299-CR06 cells with decitabine or ectopic miR-150 expression reduced viability and growth. Altogether, our results suggest that hypomethylating drugs, alone or in combination with other agents, may benefit ALK(+) patients harboring tumors resistant to crizotinib and other anti-ALK tyrosine kinase inhibitors (TKIs). Moreover, these results support further work on miR-150 in these and other ALK(+) malignancies.

Introduction

Systemic anaplastic large-cell lymphoma (ALCL) is an aggressive subtype of peripheral T cell non-Hodgkin's lymphoma derived from CD4 T cells (1, 2). WHO classification of lymphoid malignancies recognizes 2 systemic forms of ALCL, defined by the presence (+) or absence (–) of chromosomal translocations involving the anaplastic lymphoma kinase (*ALK*) gene at the 2p23 locus (3, 4).

In ALCL, the most common translocation is t(2;5)(p23;q35) that codes for the nucleophosmin-ALK (NPM-ALK) fusion protein. In addition to NPM, several other ALK translocation partners have been identified in ALK(+) ALCL. ALK fusion proteins have also been reported in other cancers, including a proportion of non–small-cell lung cancers (NSCLC) and inflammatory myofibroblastic tumors (IMTs). The ALK fusion partners induce homodimerization, leading to constitutive ALK kinase domain (KD) activation (5). Aberrant ALK activation triggers various pro-survival signaling pathways whose main target is the STAT3 pathway and subsequent oncogenesis (3, 5).

Systemic ALCL patients respond well to common first-line chemotherapy regimens such as CHOP (cyclophosphamide, hydroxy doxorubicin, Oncovin [vincristine], and prednisone). The majority of patients with NPM-ALK(+) ALCL are young and respond well to CHOP, with a long-term disease-free survival rate of over 70%. In contrast, patients with the NPM-ALK(–) disease have less than a 50% long-term disease-free survival rate with similar treatments. However, NPM-ALK(+) ALCL relapses after chemotherapy have a poor prognosis. Some patients with relapsed or refractory disease do not respond to combination therapy; for these patients, higher doses of chemotherapy followed by a stem cell transplant may be prescribed (4, 6, 7).

The dual ALK/MET inhibitor crizotinib, also known as PF2341066 or Xalkori, revolutionized perspectives on ALK-related disease management. Crizotinib was recently approved for the treatment of metastatic and late-stage ALK-rearranged NSCLC and is currently undergoing clinical trials for use in other ALK-related diseases (8, 9). Crizotinib blocks the kinase activity of ALK by binding to the ATP-binding pocket and therefore prevents the recruitment of ATP molecules. As predicted from clinical experience with other tyrosine kinase inhibitors (TKIs), mutations conferring resistance to crizotinib have already been described in ALK-associated NSCLC and in one IMT patient who had been

Conflict of interest: The authors have declared that no conflict of interest exists.
Submitted: August 11, 2014; **Accepted:** June 23, 2015.
Reference information: *J Clin Invest*. 2015;125(9):3505–3518. doi:10.1172/JCI78488.

submitted to continuous crizotinib treatment (10). A leucine-to-methionine substitution at residue 1196 (L1196M) has been shown to mediate resistance to crizotinib by impairing inhibitor binding due to steric hindrance. Leu1196 is located in the gatekeeper position at the bottom of the ATP-binding pocket. Recently, Gambacorti-Passerini and coworkers reported on the compassionate use of crizotinib administered as monotherapy to 11 ALK(+) lymphoma patients who were resistant/refractory to cytotoxic therapy (11). Crizotinib exerted a potent antitumor activity with durable responses in advanced, heavily pretreated ALK(+) lymphoma patients, with a benign safety profile. Only 2 patients progressed under short-term course continuous crizotinib treatment (11). Deep sequencing of ALK KD of these 2 patients revealed the presence of ALK mutations (11). However, no study into the long-term effects of crizotinib in ALK(+) lymphomas has been conducted. Consequently, based on the data obtained from NSCLC and IMT patients treated with crizotinib, it is highly probable that resistance would also emerge in ALCL patients, thereby limiting any further clinical benefit of crizotinib-based therapy (7, 10, 12, 13).

Recently, it has emerged that microRNAs (miRNAs) can play a role in determining drug sensitivity/resistance (14). miRNAs are endogenous small (20–23 nucleotides long) noncoding RNAs that negatively regulate gene expression at the posttranscriptional level through base-pairing interactions with their messenger RNA targets (mRNA targets). miRNAs have been found to play important roles in the regulation of the lineage differentiation fate of hematopoietic cells by modulating the expression of oncogenes or tumor suppressors. Thus, the deregulation of miRNA expression has been shown to be involved in multistep hematological malignancies and has rapidly emerged as a therapeutic target (15–19). Given that some epigenetically silenced miRNAs appear to have tumor-suppressive potential, the restoration of their expression may be an effective strategy for treating cancer (15–20). The methylation of cytosine residues within a CpG dinucleotide context by 3 members of the DNA methyltransferase (DNMT) family, DNMT1, DNMT3a, and DNMT3b, is an important epigenetic mark that mediates the repression of miRNA gene transcription (21). DNMT inhibitors such as 5-aza-2′-deoxycytidine (hereafter referred to as decitabine) cause the reexpression of methylation-silenced miRNA genes. Decitabine is a chemical cytidine analog that inhibits DNA methylation by trapping the DNMTs (22). It has been demonstrated experimentally that decitabine treatment leads to the downregulation of microRNA-target oncogenes and suppression of tumor growth (23). In addition, numerous studies have confirmed the antitumoral effects of ectopic miRNA expression using short double-stranded RNA mimics or miRNA expression vectors (24). Resistance to chemotherapy remains a major obstacle in effective anticancer treatment and results in relapse and progression in most malignant tumors. This chemoresistance may be due to drug efflux by transporters, drug inactivation by detoxification enzymes, an altered expression of proapoptosis proteins, changes in tumor-suppressor gene expression, or an increased activity of DNA repair mechanisms (25). Recent evidence has demonstrated that miRNAs play a role in all of these processes (26, 27).

Recent studies have identified a number of miRNAs aberrantly expressed in systemic ALCL patients and have suggested the involvement of miR-101, miR-29a, miR-135b, and miR-16 in mediating oncogenic NPM-ALK signaling (28–31). We have previously reported that the repression of miR-29a is dependent on the activity of both NPM-ALK and STAT3, and we demonstrated for the first time in ALCL that repression of miR-29a is likely mediated by epigenetic silencing (29). Importantly, the role of miRNAs in ALCL drug sensitivity/resistance has never been reported. We therefore sought to investigate the potential role of miRNAs in the crizotinib-response of NPM-ALK(+) ALCL, and focused our attention on miR-150.

Among the hematopoietic cell types, miR-150 is predominantly expressed in spleen and lymph nodes (32, 33). miR-150 is strongly upregulated during the differentiation of mature T cells and B cells, indicating that it might participate in B cell lymphopoiesis, T cell lymphopoiesis, or both (32, 33). In normal lymphocytes, miR-150 is thought to have a regulatory role, and the expression of miR-150 in naive cells has been shown to be rapidly downregulated after stimulation (34). miR-150 has also proven to be involved in the development of hematological malignancies (35, 36); for example, miR-150 repression has been demonstrated in an aggressive form of cutaneous T cell lymphoma (37, 38). Thus, there is now accumulating evidence that miR-150 plays essential regulatory roles in both normal and malignant hematopoiesis and holds great potential as a therapeutic target for treating various types of hematopoietic malignancies (35, 39). Honda and collaborators showed that miR-150 downregulation in scleroderma dermal fibroblasts is caused by DNA methylation and therefore can be reexpressed by decitabine treatment (40). In addition, Hassler and coworkers reported that a low dose of decitabine resulted in high antineoplastic activity in vitro and in vivo in NPM-ALK(+) KARPAS-299 ALCL cell lines and xenografted tumors (41). Thus, these data suggest that decitabine could be highly effective in treating NPM-ALK(+) ALCL and warrants further clinical evaluation for future therapeutic use. Furthermore, an aberrantly low expression of miR-150 has been identified in cutaneous T-lymphoma Sezary syndrome and in NK/T cell lymphoma. The reexpression of miR-150 in these NK/T cell lymphoma cells reduces cell proliferation, suggesting that miR-150 functions as a tumor suppressor in these cells (37). In addition, Merkel and coworkers reported that miR-150 is downregulated in various NPM-ALK(+) lymphoma models, suggesting that this miRNA may play important roles in the pathogenesis of NPM-ALK(+) ALCL (28). However, the impact of miR-150 deregulation on the oncogenic potency of NPM-ALK(+)–expressing cells has not yet been investigated. In that context, we hypothesized that repression of miR-150, caused by DNA methylation, plays a central role in the pathogenesis of T cell lymphomagenesis. To test that idea, we screened for miR-150 expression in NPM-ALK(+) human and murine lymphoma models (human NPM-ALK[+] cell lines and primary tissues, and NPM-ALK conditional transgenic mice). We show here that miR-150 expression is significantly diminished in all NPM-ALK(+) models tested. Furthermore, we show that NPM-ALK activity is responsible for miR-150 silencing in the NPM-ALK(+) ALCL cell lines. This repression is likely mediated by the epigenetic silencing of miR-150 by a DNMT1-dependent activity. In addition, DNMT1 is upregulated at the transcriptional level as a consequence of activation of the STAT3 protein, the major downstream executor of the NPM-ALK chimeric oncogenic kinase (42–44). Increasing miR-150 levels

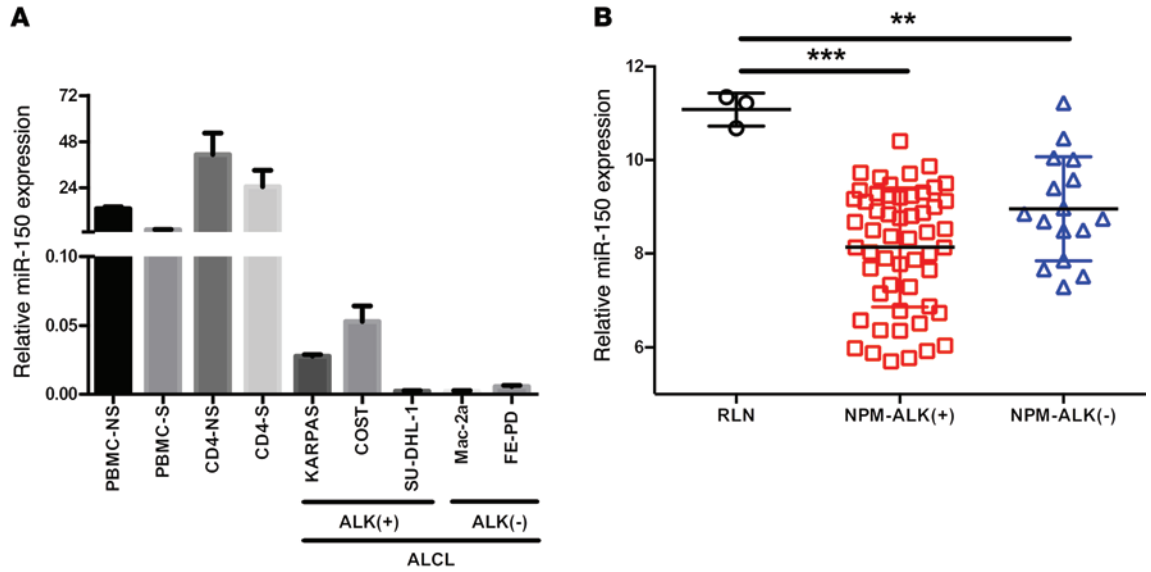

Figure 1. The expression of miR-150 is downregulated in human ALCL cell lines and biopsies. (**A**) miRNA-specific qPCR analysis of miR-150 in both PBMC and isolated CD4 lymphocytes S or NS with PHA, in 3 NPM-ALK(+) ALCL cell lines (KARPAS-299, SU-DHL-1, and COST) and 2 NPM-ALK(–) ALCL cell lines (FE-PD and Mac-2a). *RNU24* was used as an internal control. Relative miR-150 expression was expressed as the $2^{-\Delta Ct}$ relative to *RNU24*. (**B**) Microarray analysis of miR-150 expression in human NPM-ALK(+) (n = 56) and NPM-ALK(–) (n = 16) ALCL biopsies and in RLN biopsies (n = 3). Data represent mean ± SEM. $^{**}P < 0.001$, and $^{***}P < 0.0001$; unpaired 2-tailed Student's t test.

using a hypomethylating agent resulted in both downregulation of the MYB oncoprotein, a bona fide miR-150 target in hematopoietic cells, and growth inhibition of NPM-ALK(+) ALCL cells, thus providing evidence that the miR-150 pathway may be a therapeutic target for treating NPM-ALK(+) patients. Interestingly, we revealed that elevated miR-150 disadvantages the growth of crizotinib-resistant NPM-ALK(+) ALCL cells. Thus, our data strongly suggest that treatment with miRNAs could be beneficial to NPM-ALK(+) ALCL patients harboring a resistance to crizotinib and may represent a new therapeutic avenue.

Results

Aberrant miR-150 expression in NPM-ALK(+) ALCL cells. To elucidate the potential role of miRNAs in the pathogenesis of NPM-ALK(+) ALCL, Merkel et al. used a number of model systems to highlight a unique miRNA signature associated with this disease (28). In their study, miR-150 was identified as being deregulated in both human ALCL cell lines and primary tissues, as well as in the CD4/NPM-ALK transgenic mouse model (28). However, the impact of miR-150 deregulation on the oncogenic potency of NPM-ALK(+) cells was not defined. To corroborate the results of Merkel et al., we performed quantitative PCR (qPCR) to examine miR-150 levels in 3 ALCL cell lines carrying the NPM-ALK fusion protein, namely KARPAS-299, SU-DHL-1, and COST, as well as 2 NPM-ALK(–) cell lines, FE-PD and Mac-2a. miR-150 levels in these cells were compared with those in normal peripheral blood mononuclear cells (PBMC) and $CD4^+$ isolated cells stimulated (S) or not (NS) with phytohemagglutinin (PHA) (Figure 1A). These results confirmed the downregulation of miR-150 in ALK(+) cell lines. To validate that these results are relevant to primary patient cases, we measured miR-150 expression in 70 clinical samples of ALCL patients. miR-150 was shown to be significantly reduced in all human primary ALCL samples tested, as was expected due to its recognized roles in the development of hematological malignancies (refs. 35, 39, and Figure 1B). Interestingly, NPM-ALK(+) ALCL samples (n = 56) showed a greater reduction in miR-150 levels than NPM-ALK(–) samples (n = 14), when compared with reactive lymph node (RLN, n = 3) (8.13 ± 0.17 vs. 11.08 ± 0.20 for ALK[+] vs. RLN, $P < 0.0001$; 8.95 ± 0.27 vs. 11.08 ± 0.20 for ALK[–] vs. RLN, $P < 0.001$) (Figure 1B). Together, these data suggest that a proportion of the reduction in miR-150 could be an NPM-ALK–dependent phenomenon.

NPM-ALK is responsible for aberrant miR-150 accumulation in lymphoma cells. The miR-150 silencing observed in all of the NPM-ALK(+) cell lines and patient samples tested suggested that the NPM-ALK(+) protein itself might be the driving force behind this phenomenon. To test whether NPM-ALK is involved in miR-150 downregulation, NPM-ALK was silenced in 3 human NPM-ALK(+) ALCL cell lines (KARPAS-299, COST, and SU-DHL-1) using siRNAs directed against *ALK* mRNA. NPM-ALK knockdown was efficiently achieved, as shown by Western blotting (Supplemental Figure 1A; supplemental material available online with this article; doi:10.1172/JCI78488DS1). As a negative control, the same siRNAs were transfected into the FE-PD cell line, which does not express NPM-ALK. In order to check that the knockdown of NPM-ALK expression (si-ALK, Figure 2A) had been performed efficiently, we used Western blotting to detect the accumulation of the activated (phosphorylated) form of NPM-ALK (p–NPM-ALK) and STAT3 (p-STAT3) (Supplemental Figure 1A). As shown in Figure 2A, the inhibition of NPM-ALK corresponded with an increase in the expression of miR-150 in all NPM-ALK(+) cell lines. In addition, and as expected, the level of miR-150 was not modified in FE-PD cells (Figure 2A). In order to determine whether the catalytic activity of ALK can modulate miR-150 expression, we first

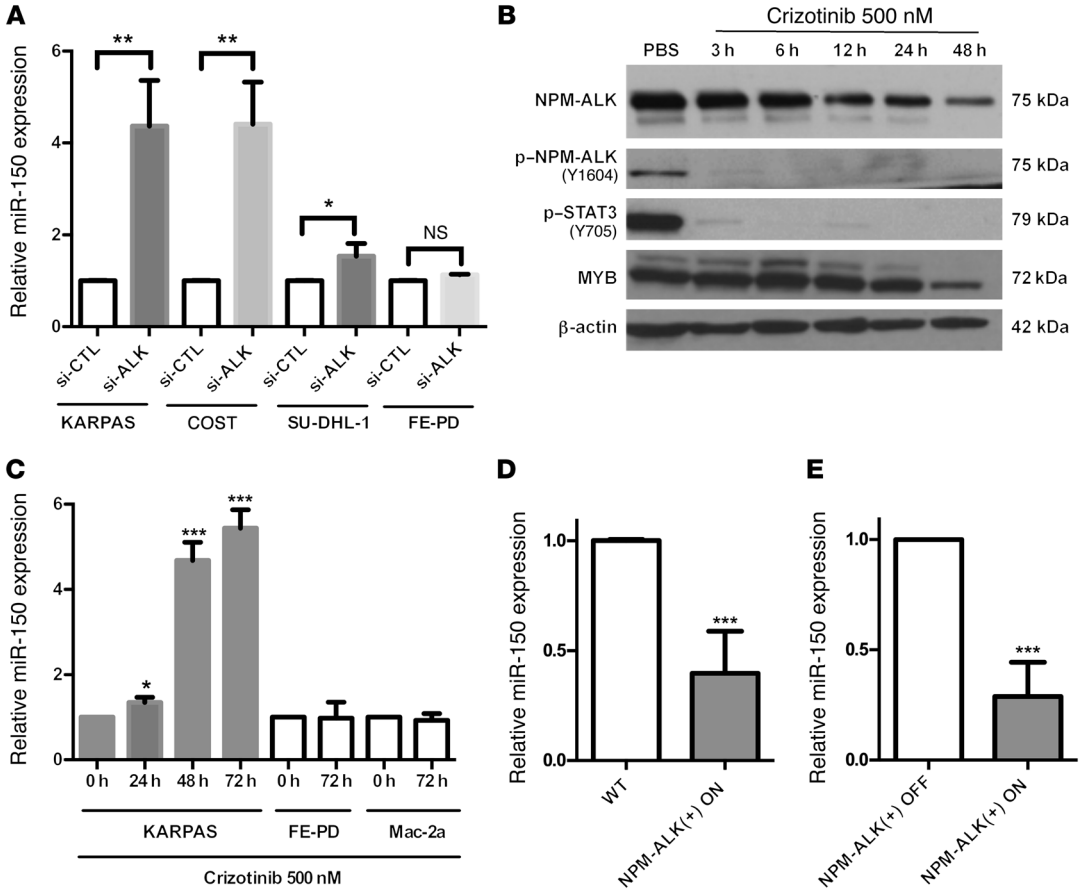

Figure 2. NPM-ALK expression promotes miR-150 downregulation. (**A**) miRNA-specific qPCR analysis of miR-150 in 3 NPM-ALK(+) ALCL cell lines (KARPAS-299, COST, and SU-DHL-1) and one NPM-ALK(–) ALCL cell line (FE-PD) transfected with either negative control siRNA (si-CTL) or si-ALK (siRNA targeting *ALK* mRNA). *RNU24* was used as an internal control. Relative miR-150 expression was expressed as the $2^{-\Delta\Delta Ct}$ relative to the si-CTL experiment. (**B** and **C**) Human KARPAS-299 cells were treated with 500 nM crizotinib for 3, 6, 12, 24, or 48 hours or with vehicle (PBS, vehicle control) for 48 hours. (**B**) Protein levels of total NPM-ALK, p–NPM-ALK (the phosphorylated form of NPM-ALK on tyrosine 1604), p-STAT3 (the phosphorylated form of STAT3 on tyrosine 705), and MYB were assessed by Western blotting using specific antibodies. β-actin served as a loading control. (**C**) miRNA-specific qPCR analysis of miR-150 in one NPM-ALK(+) ALCL cell line (KARPAS-299) and in 2 NPM-ALK(–) ALCL cell lines (FE-PD and Mac-2a) upon treatment with 500 nM crizotinib for the times shown. RNU24 was used as an internal control. Relative miR-150 expression was expressed as the $2^{-\Delta\Delta Ct}$ relative to no treatment (0 hours). (**D** and **E**) Assessment of miR-150 expression by qPCR in WT (n = 6) or NPM-ALK transgenic mice containing a Tet-OFF system. Expression of the NPM-ALK transgene was both induced (NPM-ALK[+] ON, no doxycycline, n = 8) or repressed (NPM-ALK[–] OFF, with doxycycline, n = 6), and miR-150 levels were examined in both. *SNOR202* served as an internal control, and relative miR-150 expression was expressed as the $2^{-\Delta\Delta Ct}$ relative to (**D**) WT or (**E**) NPM-ALK(–) OFF mice. Data represent mean ± SEM. n = 3; $^*P < 0.05$, $^{**}P < 0.001$, and $^{***}P < 0.0001$; unpaired 2-tailed Student's t test.

treated the KARPAS-299 cell line with either the ALK inhibitor crizotinib or with the drug vehicle alone (PBS). The loss of NPM-ALK autophosphorylation on the tyrosine 1064 residue (Figure 2B) confirmed that the ALK kinase activity was properly inhibited upon crizotinib treatment. Of note, and as expected, a decrease in STAT3 activation (p-STAT3 protein levels) was observed in parallel to ALK kinase activity inhibition (Figure 2B). Next, using qPCR, we observed that miR-150 levels were increased concomitantly to ALK tyrosine kinase inhibition (Figure 2C). In addition, the effect of crizotinib on miR-150 levels was strictly dependent on the presence of NPM-ALK, as no change was observed in FE-PD and Mac-2a cells, the NPM-ALK(–) cell lines (Figure 2C). This result suggests an ALK tyrosine kinase activity–dependent repression of miR-150 expression in NPM-ALK(+) cells.

To further investigate this finding, we took advantage of our previously published conditional NPM-ALK lymphoma transgenic mouse model (Tet-OFF-NPM-ALK murine model). miR-150 expression was assessed in the presence (NPM-ALK(–) OFF) or in the absence (NPM-ALK[+] ON) of doxycycline. In lymph nodes isolated from mice with NPM-ALK(+) lymphoma (NPM-ALK[+] ON, n = 8), we found that miR-150 was one of the most downregulated miRNAs, when compared with lymph nodes isolated from either control normal age–matched WT littermate mice (n = 6; fold change: –7.69; P = 0.01), or healthy transgenic mice who had received doxycycline treatment (NPM-ALK(–) OFF, n = 6; fold change: –3.70; P = 0.04) (F. Meggetto, unpublished observations). We then validated the expression levels of miR-150 in these samples by qPCR. miR-150 expression was significantly decreased in lymph nodes from mice with NPM-ALK(+) lymphoma, and the decrease in miR-150 levels in these cells was statistically significant when compared with cells isolated from either the lymph nodes of WT littermate transgenic

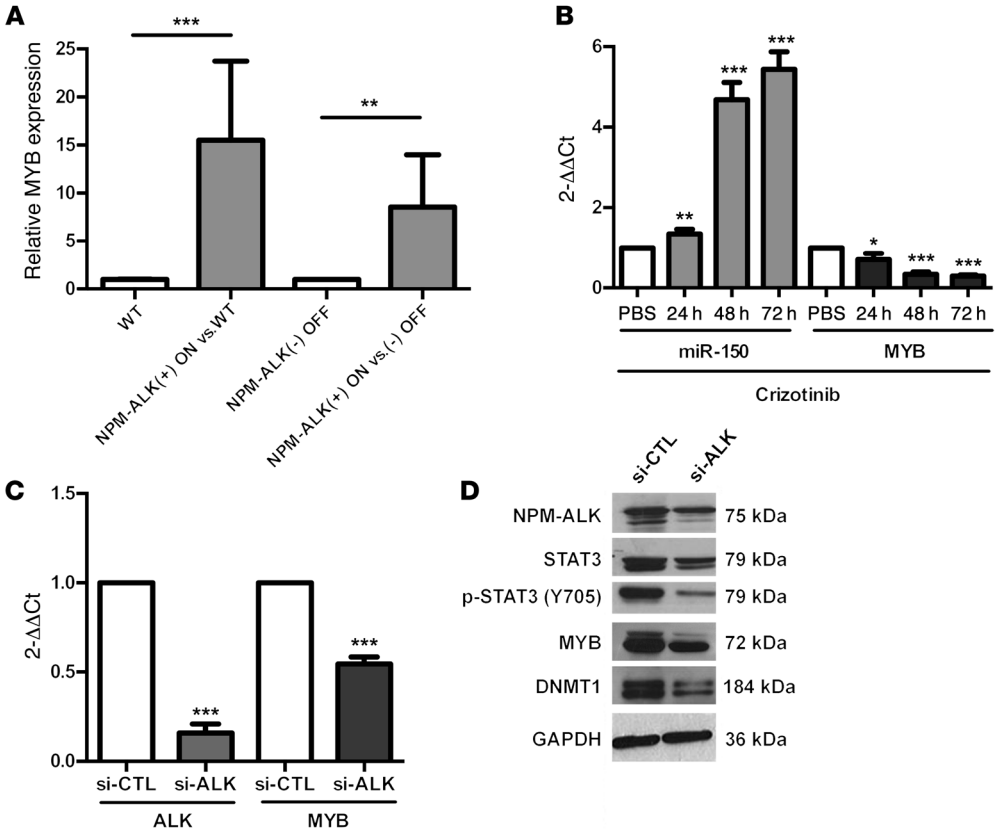

Figure 3. The miR-150 target MYB is downregulated upon NPM-ALK inhibition. (**A**) *MYB* mRNA levels were measured by qPCR in WT (n = 6) or NPM-ALK–transgenic mice upon induction (NPM-ALK[+] ON, no doxycycline, n = 11) or repression (NPM-ALK[–] OFF, with doxycycline, n = 6) of the NPM-ALK transgene. *S14* served as an internal control, and relative *MYB* expression was expressed as the $2^{-\Delta\Delta Ct}$ relative to WT or NPM-ALK(–) OFF mice. (**B**) The expression of miR-150 and *MYB* was evaluated by qPCR in KARPAS-299 cells untreated (PBS, vehicle control) or treated with 500 nM crizotinib for 24, 48, and 72 hours. miR-150 levels were normalized to those of *RNU24*, and *MYB* levels were normalized to those of *GAPDH*; these were both normalized to untreated conditions. (**C** and **D**) KARPAS-299 cells were transfected with control siRNA (si-CTL) or si-ALK. (**C**) *MYB* and *ALK* mRNA levels were analyzed by qPCR. Results were normalized to *GAPDH* and then normalized to si-CTL. Data represent mean ± SEM. n = 3; *P < 0.05, **P < 0.001, and ***P < 0.0001; unpaired 2-tailed Student's t test. (**D**) The protein levels of NPM-ALK, STAT3, p-STAT3 (form of STAT3 phosphorylated on tyrosine 705), MYB, and DNMT1 were assessed by Western blotting after knockdown of NPM-ALK. GAPDH served as an internal control to ensure equal loading.

mice (Figure 2D) or from NPM-ALK(–) OFF healthy mice (Figure 2E). Taken together, these data indicate that the NPM-ALK protein is required for maintaining a low expression of miR-150.

NPM-ALK kinase activity affects miR-150 and MYB expression. In another previous study on the transgenic mice described above, we used transcriptome analysis to compare lymph nodes from conditional NPM-ALK(+) mice (NPM-ALK[+] ON, n = 11) with normal lymph nodes from age-matched WT littermate mice (n = 6) or healthy lymph nodes from doxycycline-treated mice (NPM-ALK[–] OFF, n = 6). The induction of NPM-ALK expression was confirmed by ALK IHC and Western blotting (Supplemental Figure 2, A and B). MYB, a bona fide miR-150 target, was found to be overexpressed in murine NPM-ALK(+) lymphoma cells compared with cells isolated from the lymph nodes of normal littermate transgenic mice (fold change: 6.59; P = 0.01) or from NPM-ALK(–) OFF healthy mice (fold change: 6.60; P = 0.01) (F. Meggetto, unpublished observations; see Supplemental Methods). We then used qPCR to confirm that *MYB* was significantly overexpressed in all lymph nodes from mice with NPM-ALK(+) lymphoma compared with lymph nodes from normal littermate transgenic mice (WT) or doxycycline-treated mice (NPM-ALK[–] OFF) (Figure 3A).

To obtain insights into the relationship between NPM-ALK, miR-150, and MYB, we determined MYB expression levels under ALK knockdown conditions using KARPAS-299 cells. Both crizotinib treatment and si-ALK transfection led to a decrease in MYB at both the mRNA (Figure 3, B and C) and protein (Figure 2B and Figure 3D) levels in parallel to the induction of miR-150 expression (Figure 2A and Figure 3B). In order to check that the knockdown of NPM-ALK expression (si-ALK, Figure 3D) and activity (crizotinib, Figure 2B) had been performed efficiently, we used Western blotting to follow the accumulation of the activated (phosphorylated) form of STAT3 (p-STAT3), known to be the major downstream target of NPM-ALK. Together, these data suggest that the NPM-ALK oncoprotein affects STAT3 activation and the expression of miR-150 and MYB.

The NPM-ALK–mediated STAT3 pathway is involved in DNA methylation of the MIR150 gene. In an attempt to identify the mechanisms involved in miR-150 downregulation, we first searched for DNA loss by chromosomal studies: high-resolution array–based comparative genomic hybridization array analysis of tumoral lymph nodes from NPM-ALK conditional transgenic mice and karyotype banding in the 3 NPM-ALK(+) ALCL

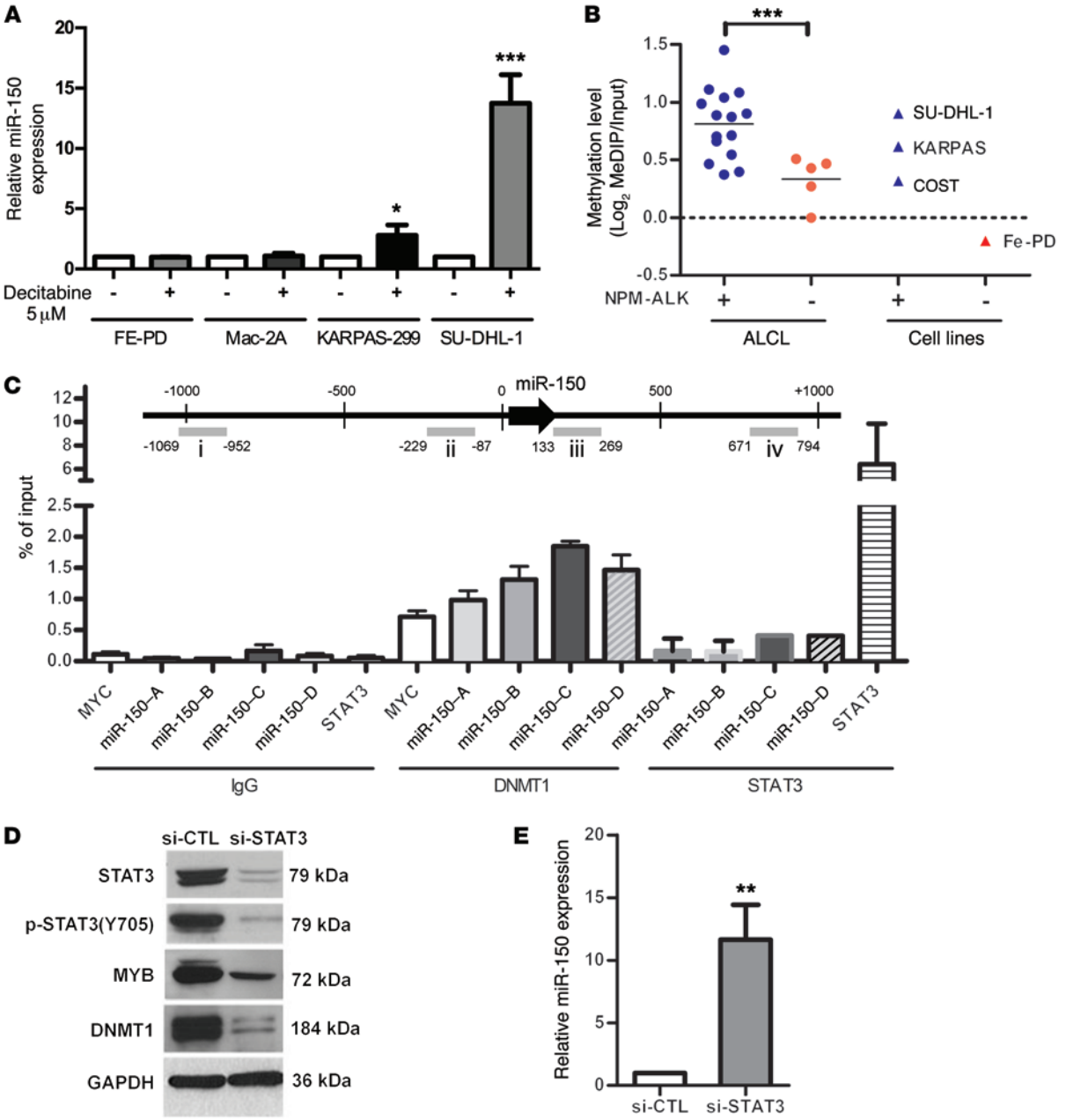

Figure 4. The expression of miR-150 is repressed in NPM-ALK(+) ALCL cells by DNA methylation. (**A**) miRNA-specific qPCR analysis of miR-150 in 2 NPM-ALK(+) ALCL cell lines (KARPAS-299 and SU-DHL-1) and 2 NPM-ALK(–) cell lines (FE-PD and Mac-2a) treated for 4 days with 5 μM decitabine. *RNU24* was used as an internal control, and relative expression of miR-150 was expressed as the $2^{-\Delta\Delta Ct}$ relative to conditions without decitabine. (**B**) Quantification of the level of DNA methylation of the *MIR150* gene from NPM-ALK(+) and NPM-ALK(–) ALCL biopsies, 3 NPM-ALK(+) ALCL cell lines (KARPAS-299, SU-DHL-1, and COST) and one NPM-ALK(–) cell line (FE-PD). (**C**) ChIP were performed using antibodies raised against DNMT1 or STAT3, or with irrelevant IgGs (as a negative control). The gDNA regions amplified are represented in the *MIR150* gene diagram (regions i, ii, iii, and iv). Results are expressed as a percentage of input. (**D**) Western blotting analysis of STAT3, p-STAT3 (form of STAT3 phosphorylated on tyrosine 705), MYB, and DNMT1 in KARPAS-299 cells transfected with control siRNA (si-CTL) or si-STAT3 (siRNA directed against *STAT3* mRNA). The GAPDH protein served as an internal control to ensure equal loading. (**E**) miR-150 expression was evaluated by miRNA-specific qPCR analysis after si-STAT3 knockdown. *RNU24* was used as an internal control, and relative miR-150 expression was expressed as the $2^{-\Delta\Delta Ct}$ relative to si-CTL conditions. Data represent mean ± SEM (bars). $n = 3$; *$P < 0.05$, **$P < 0.001$, and ***$P < 0.0001$; unpaired 2-tailed Student's t test.

cell lines: KARPAS-299, COST, and SU-DHL-1. DNA karyotype changes did not seem to be the cause of miR-150 downregulation in the NPM-ALK(+) mouse (chromosome 7) model and human (19q13.33 chromosomic region) cell lines (F. Meggetto, unpublished observations; see Supplemental Methods). As observed in these 2 NPM-ALK(+) lymphoma models, genomic hybridization array analysis shows that miR-150 downregulation in 50 ALCL patients (ALK[+] [$n = 27$] and ALK[–] [$n = 23$]) was not related to DNA deletion on the 19q13.33 region containing the independent transcription unit coding for miR-150 (L. Lamant, unpublished observations; see Supplemental Methods). In order to determine whether the observed miR-150 downregulation in NPM-ALK(+)

cell lymphomas was achieved by DNA methylation, we measured the levels of miR-150 after decitabine treatment (Figure 4A). A significant increase in miR-150 expression was observed in decitabine-treated cells compared with the drug vehicle alone in the 2 NPM-ALK(+) cell lines KARPAS-299 and SU-DHL-1. In contrast, miR-150 expression was not affected in the FE-PD and Mac-2a (ALK[–]) cell lines treated with decitabine (Figure 4A). We next analyzed the methylation status of miR-150 in a panel of 20 tumor specimens from ALCL ALK(+) and ALK(–) patients and in 4 ALCL cell lines: 3 ALK(+) (KARPAS-299, SU-DHL-1, and COST) and 1 ALK(–) (FE-PD). Using methylated DNA IP assays (MeDIP assays), with human peripheral blood T lymphocytes (PBTL) as a control, we identified a differentially methylated region of about 1 kb surrounding the miR-150 coding sequence in the NPM-ALK(+) ALCL biopsies compared with the NPM-ALK(–) biopsies and PBTL. In this region, we detected what we termed DMR (differentially methylated region), a significantly elevated level of methylation in the NPM-ALK(+) ALCL biopsies (Figure 4B and Supplemental Figure 3A). In contrast, limited methylation was detected in NPM-ALK(–) ALCL biopsies, indicating that methylation of the *MIR150* gene is an NPM-ALK–predominant phenomenon (Figure 4B and Supplemental Figure 3A). Of note, in alike biopsies, we observed a limited *MIR150* gene methylation in the NPM-ALK(–) FE-PD cell line when compared with the 3 ALCL cell lines carrying the NPM-ALK fusion, KARPAS-299, SU-DHL-1, and COST. In addition, using bisulfite sequencing, we evaluated the level of DNA methylation of the region surrounding the *MIR150* gene in KARPAS-299 and COST cells (Supplemental Figure 4A). This showed a significant level of methylation of some of the CpG dinucleotides in this region (Supplemental Figure 4B). As expected, this DNA methylation pattern was lost in cells treated with decitabine (Supplemental Figure 4B). Most importantly, we observed that the inhibition of NPM-ALK, using either crizotinib (Supplemental Figure 4C) or an siRNA targeting NPM-ALK (Supplemental Figure 4D), also induced a clear reduction in *MIR150* methylation. Finally, we confirmed that the level of miR-150, measured by qPCR, was significantly lower in NPM-ALK(+) ALCL biopsies compared with healthy RLNs (Supplemental Figure 3B).

In NPM-ALK(+) cells, 2 members of the DNMT family, DNMT1 and DNMT3b, are known to be directly responsible for the DNA methylation of microRNA genes. Therefore, we investigated whether these proteins associate with the *MIR150* gene (at locations [–]1,000 to [+]1,000 relative to the first nucleotide of pre–miR-150). Employing the KARPAS-299 cell line and a combination of ChIP and qPCR analysis (q-CHIP) with pairs of primers amplifying 4 chromatin fragments evenly distributed within the DMR region of *MIR150*, we determined that DNMT1, but not DNMT3A and DNMT3B, is markedly associated with the *MIR150* gene (Figure 4C and data not shown). As in NPM-ALK(+) cells, STAT3 is known to enhance the binding of DNMT1 to some promoters; we used q-CHIP experiments to analyze the association of STAT3 with the *MIR150* gene. As shown in Figure 4C, no STAT3 binding was observed. Finally, in NPM-ALK(+) cells, the STAT3 protein has also been shown to induce methylation of some host genes/microRNAs through transcriptional activation of DNMT1; therefore, we sought to determine the level of DNMT1 under NPM-ALK and STAT3 knockdown conditions. In si-ALK conditions, we observed, as expected, a decrease in STAT3 activation (reduced p-STAT3 protein levels) and, in parallel, a decrease in the level of DNMT1 protein (Figure 3D and Supplemental Figure 1B). In conditions of strong inhibition of STAT3 in KARPAS-299 (compared with its inhibition via si-ALK, Figure 3D), DNMT1 protein levels were decreased (Figure 4D), with a concomitant increase in miR-150 expression (Figure 4E). The levels of the DNMT1 protein were also evaluated in the conditional NPM-ALK lymphoma transgenic mouse model. As shown in Supplemental Figure 2B, DNMT1 is markedly overexpressed in NPM-ALK(+) ON mice compared with WT or NPM-ALK(–) OFF mice. Thus, the downregulation of miR-150 in NPM-ALK(+) cell lymphomas is likely to be regulated, at least in part, by epigenetic silencing via STAT3 and DNMT1 activation.

Ectopic expression of miR-150 inhibits proliferation and blocks S-phase entry of NPM-ALK(+) cells in vitro. To investigate the effect of miR-150 on cell proliferation, we transfected the NPM-ALK(+) cell line KARPAS-299 with miR-150 microRNA mimics. The successful overexpression of miR-150 in the cells was confirmed by qPCR (Supplemental Figure 5). Using Western blotting, we checked that the expression of MYB, a bona fide miR-150 target, was reduced in NPM-ALK(+) cells transfected with miR-150 (Figure 5A). MTS and colony-formation assays showed that ectopic expression of miR-150 could markedly inhibit cell viability (Figure 5B) and block clonogenicity (Figure 5, C and D) of NPM-ALK(+) cells compared with the mimic microRNA control (miR-CTL). This antiproliferation effect could be partially due to the disruption of cell growth regulation, such as cell cycle arrest. Thus, we next explored the effect of miR-150 on cell cycle regulation. Flow cytometric cell cycle analysis showed that miR-150 transfection in KARPAS-299 NPM-ALK(+) ALCL cells increased the number of cells in G0/G1 phase and decreased the number of cells in S and G2/M phases of the cell cycle compared with miR-CTL transfection (Figure 5E). There was no detectable increase in the sub-G0/G1 fraction. Accordingly, we noted the lack of an increase in apoptosis (7AAD/Annexin-V staining, data not shown), which was further supported by the absence of a detectable increase in the cleaved caspase–3 level shown on Western blots (data not shown). In addition, we observed that the mitotic index was markedly different between KARPAS-299 cells with ectopic miR-150 expression (1.8% of cells) and those expressing miR-CTL (7%) (Figure 5F). In addition, we could show that the ectopic expression of miR-150 induces a decrease of the MYB protein level (Supplemental Figure 6A) and affects the in vitro growth of the COST cells, another NPM-ALK(+) ALCL cell line (Supplemental Figure 6, B and C). All these results suggest that miR-150 has a key role in the growth of NPM-ALK(+) cell lines, it attenuates MYB expression, and it works as a tumor suppressor.

The overexpression of miR-150 hampers the growth of NPM-ALK(+) ALCL in vivo. We next investigated the efficiency of miR-150 transfection on tumor growth of 2 NPM-ALK(+) ALCL cell lines in vivo (KARPAS-299 and COST). miR-CTL– or miR-150–transfected KARPAS-299 or COST cells were inoculated s.c. into the left or right flank of each mouse, respectively (n = 5 for KARPAS-299 and n = 6 for COST). Transfection of miR-150

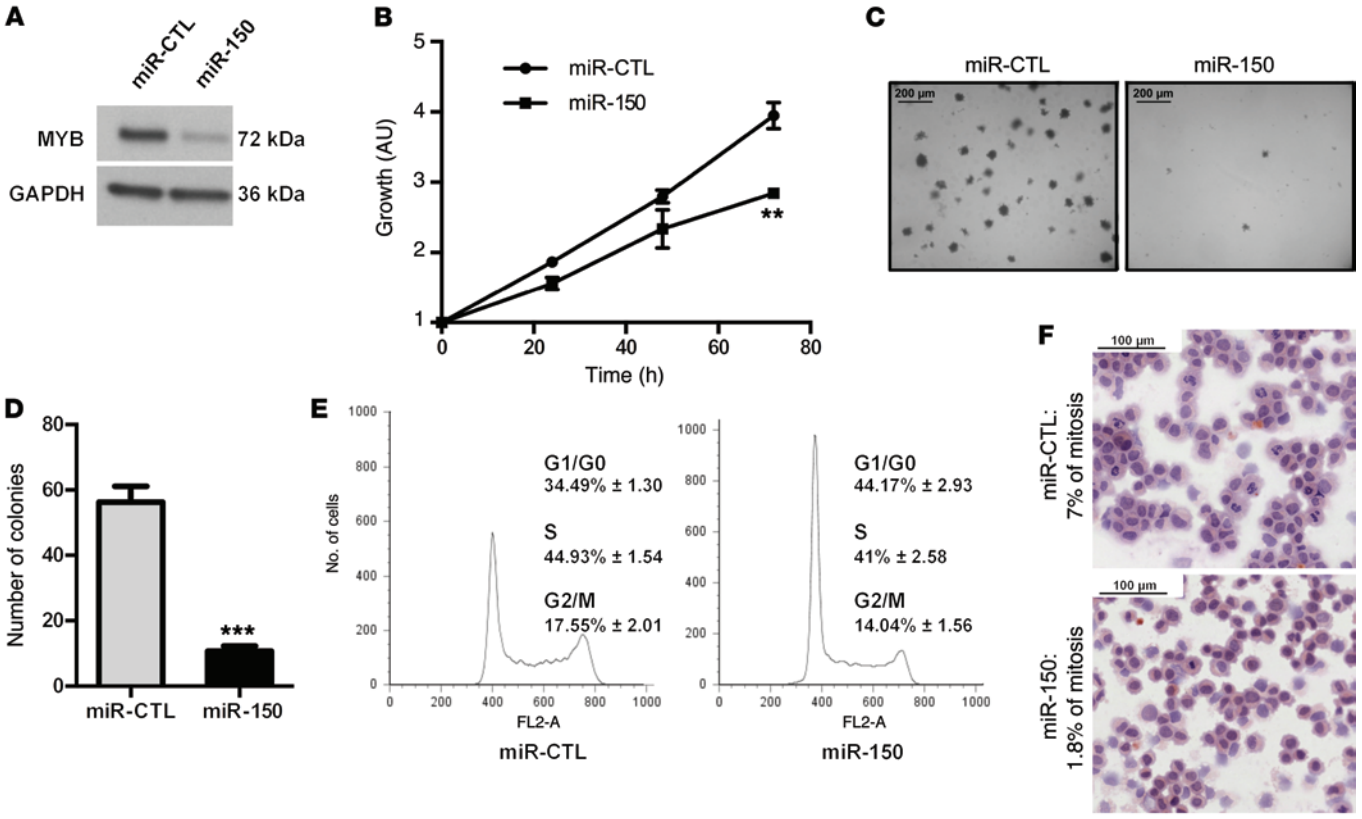

Figure 5. miR-150 overexpression inhibits proliferation and promotes G1 arrest of KARPAS cells in vitro. (**A**) Western blotting analysis of MYB protein levels after transfection of KARPAS-299 cells with miR-CTL or miR-150 microRNA mimics. GAPDH served as an internal control to ensure equal loading. (**B**) MTS colorimetric measurement of cell viability after miR-CTL or miR-150 transfection in KARPAS-299 cells. (**C** and **D**) Soft agar assay for anchorage-independent cell growth of miR-CTL– and miR-150–transfected KARPAS-299 cells. Picture of the plate (scale bars: 200 μm, original magnification ×10) (**C**) and quantification of the number the colonies (**D**) using ImageJ software. (**E**) Cell cycle analysis of miR-CTL– and miR-150–transfected KARPAS-299 cells (with propidium iodide incorporation measured by FACS on a FACSCALIBUR). Data represent mean ± SEM. $n = 3$; $^{**}P < 0.001$, and $^{***}P < 0.0001$; unpaired 2-tailed Student's t test. Each experiment was repeated 3 times. (**F**) Hematoxylin and eosin staining of miR-CTL– and miR-150–transfected KARPAS-299 cell cytospins (scale bars: 100 μm, original magnification ×20). For each condition, the number of mitotic cells was determined for a sample of 500 cells ($n = 2$).

into KARPAS-299 and COST cells resulted in decreased growth and tumor weight of s.c. xenograft tumors in NOD/SCID mice when compared with those transfected with miR-CTL (Figure 6, A–C). Morphological analyses showed that forced expression of miR-150 caused phenotypic hallmarks of cellular degeneration (uncommon chromatin condensation, nuclear piknosis, cellular volume decrease, and nuclear envelope disruption) (Figure 6D). These results show that miR-150 overexpression drastically disadvantages the growth of NPM-ALK(+) cells in vivo.

Demethylating treatment or ectopic miR-150 expression correlates with growth inhibition of crizotinib-resistant NPM-ALK(+) ALCL cells. KARPAS-299-CR06 cells express a form of NPM-ALK presenting the substitution mutation L1196Q within the KD. This NPM-ALK mutant is insensitive to the crizotinib inhibitor and, therefore, no change in STAT3 activation is observed upon crizotinib treatment (Supplemental Figure 7A). We examined the expression level of miR-150 in crizotinib-resistant KARPAS-299-CR06 cells. miR-150 was found to be significantly downregulated in KARPAS-299-CR06 cells compared with parental KARPAS-299 cells (Supplemental Figure 7B). In order to examine the possible role of miR-150 in crizotinib-resistance, we first induced an increase in miR-150 expression with decitabine (Supplemental Figure 7C). We examined the effect of crizotinib treatment or a combination of the 2 agents (crizotinib + decitabine) on miR-150 expression. A significant increase in miR-150 expression was observed in crizotinib-treated CR06 cells upon decitabine treatment compared with untreated cells or cells only treated with crizotinib (Supplemental Figure 7C). Subsequently, we analyzed cell growth. As expected, crizotinib had no inhibitory effect on viability and on the ability of KARPAS-299-CR06 cells to form colonies (Figure 7, A and B, and Supplemental Figure 8A), in accordance with the more aggressive phenotype of these cells compared with the more sensitive parental KARPAS-299 cells. In contrast, decitabine markedly reduced cell viability and blocked clonogenicity in soft agar assays (Figure 7, A and B, and Supplemental Figure 8A). The same results were obtained after the addition of decitabine and crizotinib (Figure 7, A and B, and Supplemental Figure 8A). Thus, resistance to crizotinib due to NPM-ALK substitution mutation does not confer cross-resistance to decitabine and does not affect the antiproliferative activity of the demethylating drug in KARPAS-299-CR6 cells treated with the drug alone or in combination with crizotinib. Since the hypomethylating agent caused miR-150 overexpression in these crizotinib-resistant NPM-ALK(+) cells

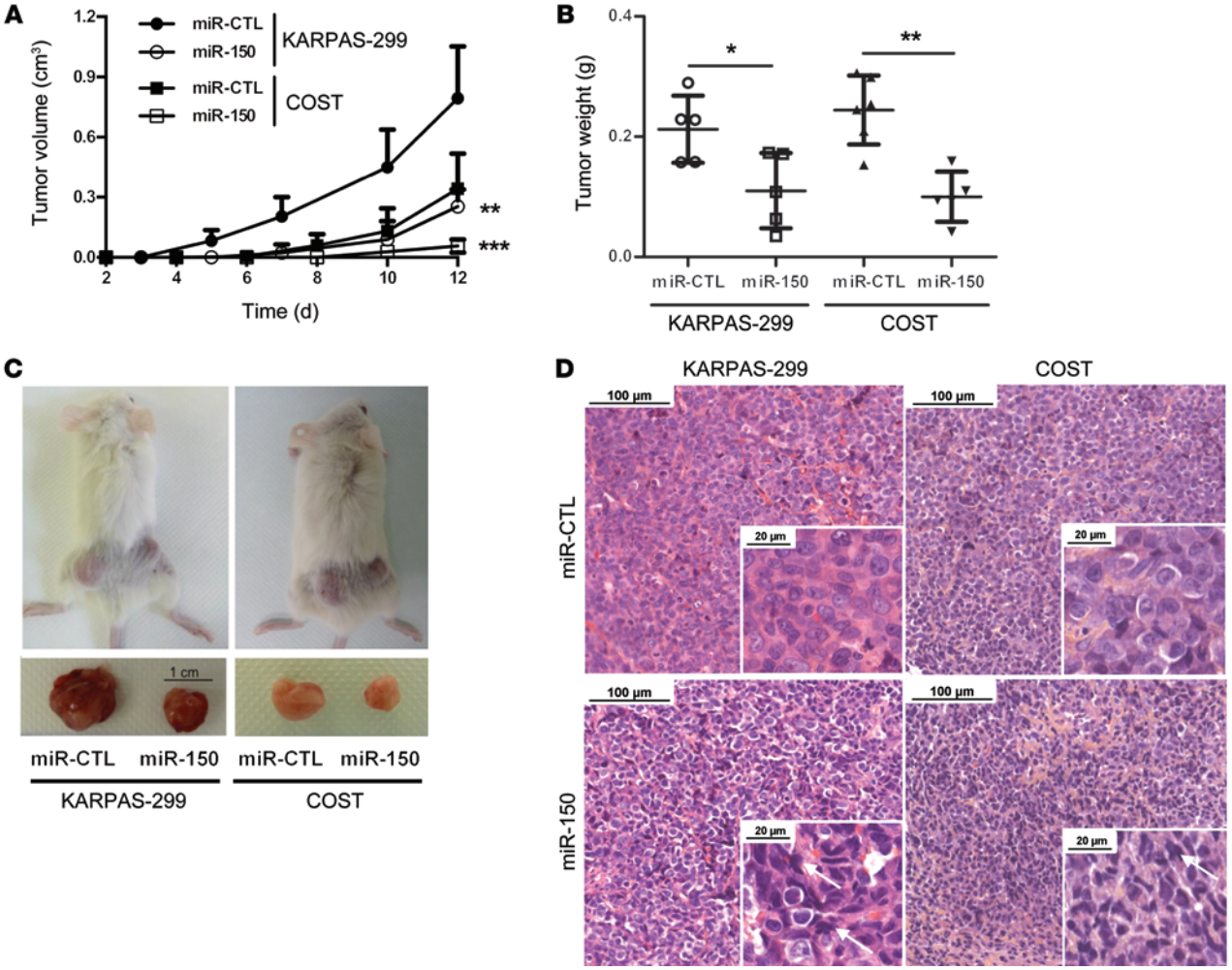

Figure 6. miR-150 overexpression inhibits KARPAS-299 and COST xenograft growth in NOD/SCID mice. (**A**) NPM-ALK(+) KARPAS-299 and COST cells transfected either with miR-CTL or miR-150 were injected s.c. in the left or right flank of 5 NOD/SCID mice, respectively (n = 5). Tumor volume was evaluated over time by caliper measurements and reported as mean ± SEM (bars). $^{**}P < 0.001$, $^{***}P < 0.0001$, using unpaired 2-tailed Student's t test. (**B**) Tumor weight measurement, reported as mean ± SEM (bars). $^{*}P < 0.05$, $^{**}P < 0.001$, using unpaired 2-tailed Student's t test. (**C**) Representative tumors resected from mice xenografted with miR-CTL– or miR-150–transfected KARPAS-299 and COST cells. Scale: 1 cm. (**D**) Micrographs of hematoxylin and eosin staining of excised miR-CTL or miR-150 tumors (scale bars: 100 μm, inset 20 μm; original magnification ×20, inset ×80). Arrows indicate cells with phenotypic hallmarks of cellular degeneration, i.e., uncommon chromatin condensation, nuclear piknosis, cellular volume decrease, or nuclear envelope disruption.

(Supplemental Figure 7C), we considered that addition of miR-150 could disadvantage the growth of these cells. To investigate this hypothesis, we transfected miR-150 mimics into KARPAS-299-CR06 cells. MTS and colony-formation assays showed that the ectopic expression of miR-150 not only markedly inhibited cell viability (Figure 7D), but also had a large inhibitory effect on the number of colonies formed (Figure 7E and Supplemental Figure 8B) and blocked S-phase entry (Supplemental Figure 8C) in crizotinib-resistant NPM-ALK(+) cells compared with those transfected with the microRNA mimic control. Importantly, as with demethylating treatment (Figure 7C), we observed that ectopic miR-150 expression also corresponded to a large antiproliferative effect that attenuated MYB expression in these crizotinib-resitant NPM-ALK(+) cells (Figure 7, C and F). The same results were obtained in KARPAS-299-CR6 cells when STAT3 activity was blocked by the small-molecule inhibitor Stattic, or when siRNAs directed against *STAT3* mRNA were used in combination with decitabine (Supplemental Figure 9). All of these results suggest that the restoration of miR-150 could inhibit the growth of crizotinib-resistant NPM-ALK(+) ALCL cells.

Discussion

Epigenetic gene silencing plays an important role in carcinogenesis. By inhibiting the expression of many tumor-suppressor genes, DNA methylation of gene promoter regions is a key component of this process (45). DNA methylation is also an important epigenetic mechanism for silencing genes transcribed by RNA polymerase II, including miRNA genes (15, 18, 19). Recent reports have shown that miRNAs undergo the same epigenetic regulatory laws as any other protein-coding genes (20, 46, 47). Methylation is mediated by members of the DNMT family that can be inactivated by small-molecule inhibitors such as decitabine (22). High DNMT1 expression is found in human ALCL cell lines and primary tumors (41). In NPM-ALK(+) ALCL cell lines, transcription of the

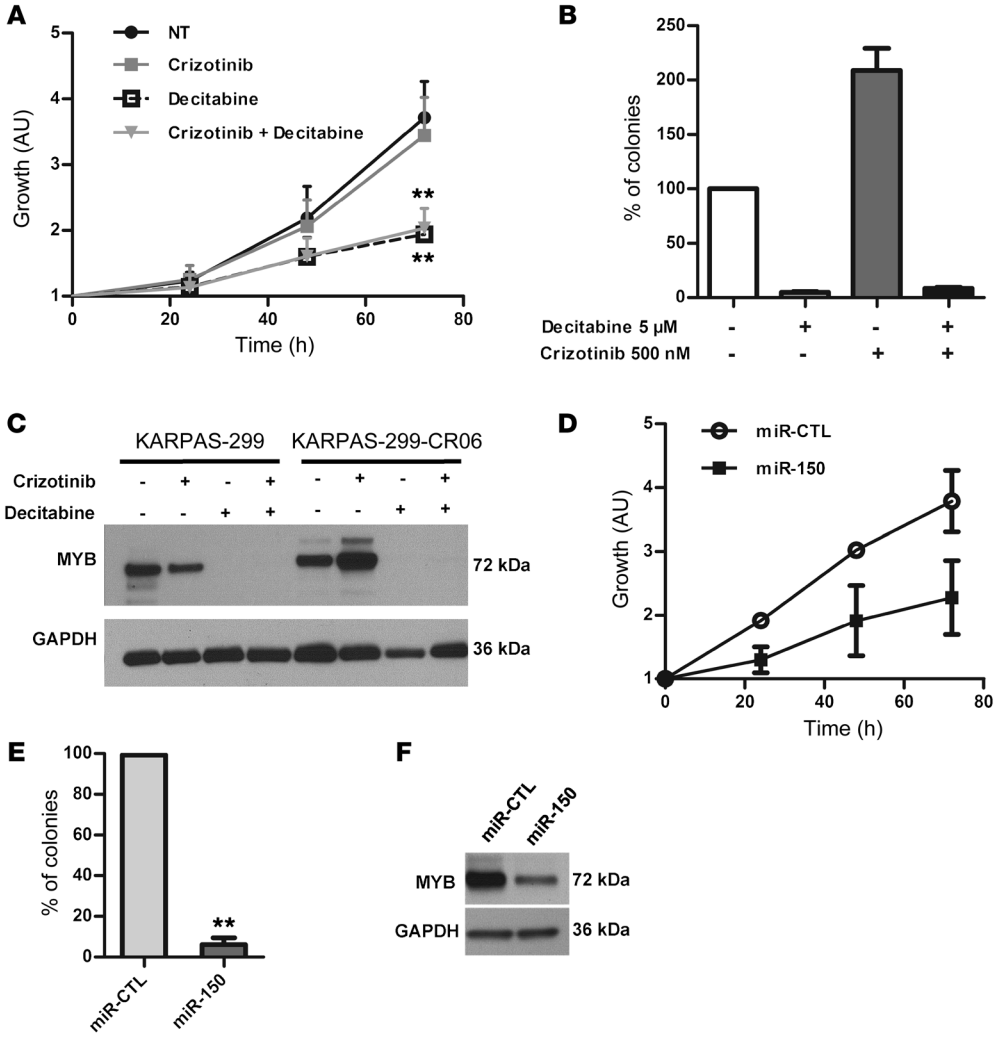

Figure 7. Decitabine treatment, via the STAT3/miR-150/MYB axis, inhibits growth of the crizotinib-resistant KARPAS-299-CR06 mutant. (**A** and **B**) MTS colorimetric measurement of cell viability (**A**) and soft agar assay for anchorage-independent cell growth (**B**) of crizotinib-resistant KARPAS-299-CR06 cells untreated or treated with 500 nM crizotinib and/or 5 μM decitabine. (**C**) Western blotting shows expression of MYB in crizotinib-resistant KARPAS-299-CR06 cells and crizotinib-naive KARPAS-299 parental cells (KARPAS-299). (**D** and **E**) MTS colorimetric measurement of cell growth (**D**) and soft agar assay (**E**) of crizotinib-resistant KARPAS-299-CR06 cells transfected with either miR-CTL or miR-150. Data represent mean ± SEM. $n = 3$; $^{**}P < 0.001$; unpaired 2-tailed Student's t test. (**F**) Evaluation of MYB expression in miR-CTL– or miR-150–transfected KARPAS-299-CR06 cells by Western blotting.

DNMT1 gene is induced by STAT3, which functionally interacts with DNMT proteins and thereby encourages promoter hypermethylation and gene silencing (48–51). In a previous study, we showed that the STAT3/DNMT1 axis mediates miRNA epigenetic silencing in NPM-ALK(+) ALCL cells (29). Now in the present work, we describe how miR-150 is partly repressed by methylation in an NPM-ALK–dependent pathway via STAT3 activation and DNMT1 expression. We did not observe any cooperation between the STAT3 transcription factor and DNMT1 at the miR-150 locus. Until now, only one study has shown that miR-150 downregulation is caused by repressive DNA methylation in human autoimmune diseases and that, therefore, miR-150 can be overexpressed through decitabine treatment (40). Although the efficacy of decitabine in solid tumors is limited, this drug is the most widely investigated demethylating agent (52) and is approved by the US FDA for use as a monotherapeutic agent against hematological cancers (53), such as in the treatment of myelodysplastic syndrome (54, 55). Clinical responses appear to be induced by both epigenetic alterations and the induction of cell cycle arrest and/or apoptosis (56). Decitabine is a potent DNMT inhibitor, but unfortunately, its effect is transient because of its instability. Using drug-resistant cell lines, which included leukemia models, Vijayaraghavalu and coworkers reported that sustained DNMT1 depletion prolonged cell arrest in the G2/M cell cycle phase and significantly enhanced the antiproliferative effect of decitabine (57). They also showed that the efficacy of decitabine was more significant in resistant cells than in sensitive cells. These data suggest that effective delivery of decitabine and prolonged DNMT1 depletion are critical to overcome drug resistance (57).

Only one study has demonstrated that decitabine exhibits an antineoplastic activity against NPM-ALK(+) ALCL cells and xenografted tumors both in vitro and in vivo (41). It is thus tempting to propose that decitabine could be an effective treatment against NPM-ALK(+) ALCL, possibly through causing miR-150 reexpression. In NPM-ALK(+) KARPAS-299 ALCL cells, we observed that miR-150 expression was increased upon decitabine treatment. In vivo, upregulation of miR-150 expression exhibited an antineoplastic activity against xenografted NPM-ALK(+) KARPAS-299 tumors. The overexpression of miR-150 induced a significant decrease in the number of viable cells, and cell cycle analysis showed a decrease in the proportion of cells in S phase as well as G2/M phase. This cell cycle blockage was not associated with an increase in apoptosis, similar to that reported by Han and coworkers, who also treated KARPAS-299 cells with decitabine (16). Moreover, in NPM-ALK(+) KARPAS-299 ALCL cells, we observed that upregulation of miR-150

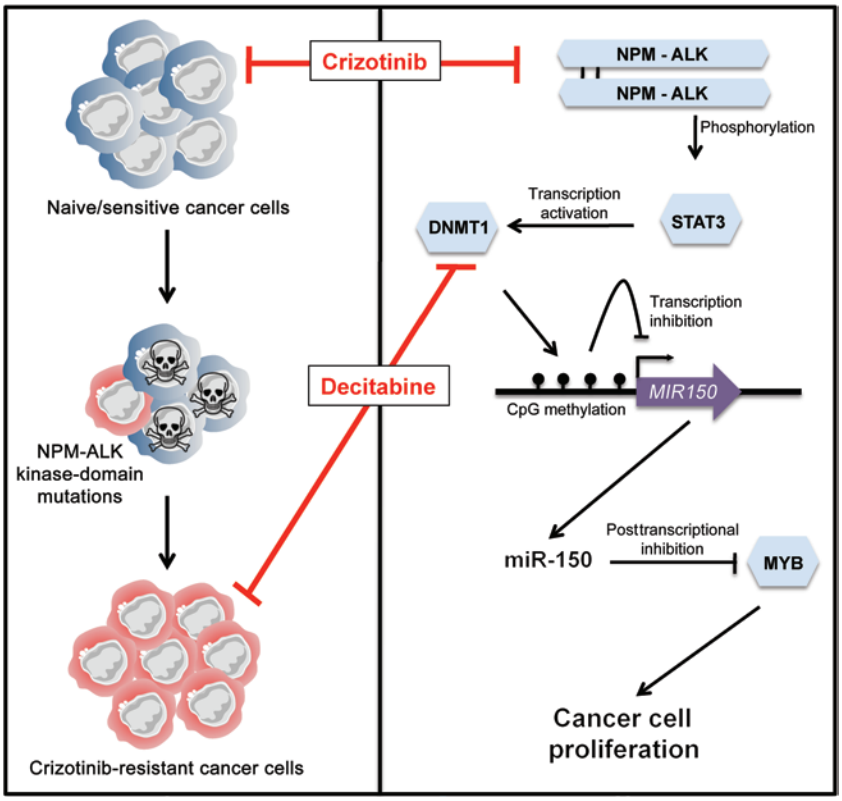

Figure 8. Schematic model of the NPM-ALK/STAT3/DNMT1/miR-150/MYB regulatory circuit in NPM-ALK(+)-associated lymphomas. In naive/sensitive cells and cells resistant to crizotinib (an ALK TKI), the NPM-ALK fusion protein inhibits the expression of miR-150 through a DNA methylation mechanism that is dependent on the STAT3 and DNMT1 proteins. In naive/crizotinib-sensitive NPM-ALK(+) cells, crizotinib or demethylating drugs such as decitabine repress the STAT3/DNMT1 axis, thus releasing miR-150 inhibition and reducing the level of its target gene, MYB. These changes, in turn, result in decreased cell proliferation and lead to lymphoma growth inhibition. Concomitantly to its large antiproliferative effect, miR-150 expression also attenuates MYB expression in crizotinib-resistant NPM-ALK(+) cells harboring a substitution mutation within the ALK KD. These findings should promote further investigation into the effect of epigenetic modulation in other ALK-related malignancies harboring either different mutation types, different ALK fusions, or overexpressed/activated ALK full-length oncogenes. Illustration created by Servier Medical Art (http://www.servier.fr/servier-medical-art).

resulted in a significant downregulation of MYB, an important miR-150 target. Altogether, our findings suggest that miR-150 overexpression leads to a drastic inhibition of cell growth and tumor formation through repression of the downstream target MYB, a master regulator of proliferation (Figure 8; refs. 58–60). Indeed, it is a known fact that, in NPM-ALK(+) ALCL cells, the functional effects of MYB are modulated by transcription factors and cell cycle proteins, which include MYC and cyclin-D1 (60–62). The promoters of *MYC* and cyclin-D1 are MYB targets, and their mRNA is stabilized by the AUF1/hnRNPD protein in NPM-ALK(+) KARPAS-299 ALCL cells (63, 64); however, we did not observe links between MYB, MYC, and cyclin-D1 protein expression in an miR-150–dependent context (data not shown). As an aside, since MYC blocks miR-150 expression in acute myeloid leukemia (65) and can repress transcription through recruitment of a DNA methyltransferase corepressor to turn off DNA methylation of promoters (66), we also investigated whether MYC associates with the *MIR150* gene and could also participate in miR-150 silencing in NPM-ALK(+) cells. Using ChIP assays in NPM-ALK(+) KARPAS-299 ALCL, we did not observe MYC binding to the miR-150 locus (data not shown).

Drug resistance is a major obstacle for the successful treatment of cancer. Aberrant expression of DNMTs is recognized as a key factor in the onset of cancer and drug resistance. The DNMT1 protein promotes DNA methylation to maintain cancer-drug resistance. In solid tumors, high levels of DNMT1 have been reported in cancer patients insensitive to chemotherapy (67). Thus, sustained DNMT1 depletion is a potential target for overcoming drug resistance. Although the majority of ALK(+) patients respond to polychemotherapy, the standard treatment for ALCL, new treatments are needed for resistant or relapsing patients (3, 7, 68, 69). The use of crizotinib, an ALK TKI, has revolutionized the treatment of ALK(+) patients with advanced-stage or relapses (70). However, acquired resistance, defined as progression after initial benefit, inevitably occurs upon such targeted treatment (10, 71). Although drug resistance can be overcome using epigenetic therapies in experimental models, clinical studies have highlighted the challenges of current epigenetic therapies for solid tumors and the need to identify more targeted approaches (72). From this has arisen the potential of hypomethylating agents, such as decitabine, which have been assessed to be able to cooperate with TKIs (22). Ceccon and coworkers generated a stable subpopulation of KARPAS-299 cells that are able to live and proliferate in the presence of crizotinib, naming them CR06 (for crizotinib resistant growing with 600 nM of crizotinib) (73). KARPAS-299-CR06 cells express a form of NPM-ALK presenting the substitution mutation L1196Q within the KD. A leucine substitution in residue position 1196 is found at relatively high frequency in NSCLC patients. This mutation was shown to confer resistance to the drug in vitro. Interestingly, Leu1196 corresponds to a key residue that has been observed to confer resistance to many TKIs (10). The same position is exploited by BCR-ABL (the most infamous T315I mutant, ref. 74) to enable it to survive TKI therapy, and the corresponding EGFR T790M mutation gives complete resistance to EGFR (75).

We have shown that this NPM-ALK–gatekeeper mutation, at the Leu1196 position, does not confer cross-resistance to decitabine and does not affect the antiproliferative activity of decitabine on KARPAS-299-CR06 cells. Using crizotinib-resistant KARPAS-299-CR06 cells, we identified that restoration of miR-150 by

decitabine could disadvantage the growth of the crizotinib-resistant NPM-ALK(+) cells. As for crizotinib-naive or -sensitive NPM-ALK(+) cells, the response to decitabine appears to be induced by modifications at both the miR-150 and MYB levels, and cell cycle arrest was induced with no significant increase in apoptosis. To the best of our knowledge, our study reveals for the first time that hypomethylating/antileukemic drugs show great potential for the treatment of crizotinib-resistant ALK(+) cells (Figure 8). In accordance with our findings, La Rosée and coworkers used resistant cell lines caused by the expression of mutated Bcr-Abl to demonstrate in vitro that combined treatment with decitabine and imatinib, a selective inhibitor of the BCR-ABL tyrosine kinase, is beneficial for imatinib-resistant cells (76). Clinical trials are now underway to determine whether these results are valid in a physiological environment.

The discoveries of the EML4-ALK fusion in 2007 as the oncogenic driver in NSCLC and then the identification of activating mutations of the *ALK* gene in the development of neuroblastoma have made ALK one of the most extensively studied targets in the field of TKI drug development (77–80). Our findings suggest that an alternative option in these cases would be to target deregulated epigenetic mechanisms and apply decitabine in combination with already-established drugs, such as crizotinib or other ALK inhibitors, to TKI-resistant ALK(+) tumors or in combination with other agents to improve the overall response rates without exposing patients to long-term toxicities. Consequently, our study should promote further investigation into the effect of epigenetic modulation in other ALK-related malignancies that harbor either different ALK fusions or overexpressed/overactivated full-length *ALK* oncogenes.

Methods

Human cell lines, and tumoral and normal samples. KARPAS-299, COST, and SU-DHL-1 ALK(+) ALCL cell lines bearing the t(2;5)(p23;q35) translocation were obtained from DSMZ (German Collection of Microorganisms and Cell Culture) or established in our laboratory. Both the ALK(–) ALCL cell lines, Mac2a and FE-PD, were provided by O. Merkel (Medical University, Vienna, Austria) and K. Pulford (Oxford University, Oxford, United Kingdom) respectively, as gifts. Cells were cultured in Iscove Modified Dulbecco's medium (IMDM, Invitrogen) supplemented with 15% FCS and were maintained in exponential growth phase. The KARPAS-299-CR06 cell line was provided by C. Gambacorti-Passerini and M. Ceccon (Department of Health Sciences, University of Milano-Bicocca, Milan, Italy) (73) and was cultured in RPMI-1640 supplemented with 10% FCS. Medium was replaced with fresh RPMI-1640 supplemented with 600 nM crizotinib every 48 or 72 hours. PBMCs from 3 healthy donors were used as normal lymphoid cells and were provided by A. Quillet-Mary (UMR1037, CRCT). PBMCs and $CD4^+$ isolated cells were stimulated using 3 μg/ml PHA for 96 hours in RPMI-1640 with 10% FCS. All cells were cultured at 37°C with 5% CO_2, and all media were supplemented with 2 mM L-glutamine, 1 mM sodium pyruvate, and 100 U/ml penicillin/streptomycin (all from Invitrogen).

Tumor samples from 56 ALK(+) ALCL, 14 ALK(–) ALCL, and 3 RLNs were retrieved from our tumor tissue bank. The diagnosis of ALCL was based on morphologic and immunophenotypic criteria, as described in the last WHO classification. The percentage of malignant cells was assessed by ALK1 or CD30 staining and was greater than 50% for all selected cases. Antibody binding was detected with the Dako REAL Detection System (Code K5001).

Cell treatments. NPM-ALK, STAT3, and DNMT1 activities were inhibited using, respectively, 500 nM of crizotinib (@rtMolecule) for 3–96 hours, 5 μM Stattic (Sigma-Aldrich) for 48 hours, and 5 μM of decitabine (Sigma-Aldrich) for 96 hours. The final concentration of Stattic and decitabine used throughout this study was based on the findings of a previous study (16, 81). Decitabine was added to the cell culture daily in order to maintain a constant concentration. Crizotinib was synthetized and purchased at @rtMolecule (France). KARPAS-299-CR06 cells were treated with 600 nM of crizotinib for 12 hours after microRNA mimic transfection.

ChIP. ChIPs were done using SimpleChIP Plus Enzymatic Chromatin IP Kit (Magnetic Beads, Cell Signaling) according to the manufacturer's instructions. The optimal ChIP conditions were obtained using 7×10^6 of KARPAS-299 cells and 1,000 gel units of micrococcal nuclease for each IP performed (Supplemental Table 2). The ChIP and Input (2% of the starting material) samples were analyzed by qPCR (Supplemental Table 1). Results are expressed as percentage of input ($100*2\text{^}[(Ct_{input}-[\log2 \text{ of } 50]) - Ct_{ChIP}]$).

Bisulfite sequencing. Genomic DNA (gDNA) extraction, bisulfite conversion, and Illumina sequencing were performed by Active Motif (http://www.activemotif.com). gDNA was extracted from 3 million KARPAS-299 cells treated for 5 days with 5 μM decitabine or 500 nM crizotinib, and 3 million COST cells transfected with si-RNA targeting NPM-ALK. gDNA samples were then subjected to bisulfite conversion. PCR amplicons were generated using forward and reverse bisulfite primers (Supplemental Table 1) designed to amplify a 541-bp region of the *MIR150* gene containing 22 CpG dinucleotides. PCR products were sequenced on Illumina NextSeq 500. As reference sequence, the human chr19 (hg19 assembly) was used.

Statistics. Differences between 2 groups were examined using 2-tailed Student's *t* test. All analyses were performed using GraphPad Prism version 6.00 for Windows. $P < 0.05$ was considered significant.

Study approval. Frozen tumor samples were retrieved from CHU de Toulouse tumor tissue bank. The study was carried out in accordance with the institutional review board–approved protocols, and the procedures followed were in accordance with the Helsinki Declaration of 1975, as revised in 2000. Mice were housed under specific pathogen-free conditions, in a constant temperature (20°C–22°C) animal room, with a 12-hour light/12-hour dark cycle and free access to food and water. All animal procedures were performed following the principle guidelines of INSERM, and our protocol was approved by the Midi-Pyrénées Ethics Committee on Animal Experimentation.

Accession number. Bisulfite sequencing data were deposited to the Gene Expression Omnibus (GEO) public database according to MINSEQE standards (accession no. GSE69836).

Acknowledgments

This work was supported by grants from the INSERM, Fondation ARC pour la Recherche sur le Cancer (to F. Meggetto), the Fondation de France (to F. Meggetto), INCa-projet PAIR Lymphomes (to L. Lamant), and The Institut Universitaire de France (to P. Brousset). C. Hoareau-Aveilla was under a contract supported by Fondation pour la Recherche Médicale and Fondation de France; T. Valentin was supported by a fellowship from Plan Cancer 2009–

2013/Soutien 2012 à l'ITMO Cancer/Soutien pour la formation à la recherche translationnelle en cancérologie 2012; and C. Daugrois by the Labex TOUCAN/Laboratoire d'excellence Toulouse Cancer. For their technical assistance, the authors thank M. Foisseau (CRCT/INSERM/UMR1037), F. Capilla, C. Salon, and T. Al Saati at the histology facility of INSERM/UPS-401 US006/CREFRE (Toulouse, France); F. L'Faqihi and V. Dupan at the flow cytometry facility of INSERM/UMR1043 (Toulouse, France); C. Demur (Laboratoire d'hématologie, IUCT Oncopole) and I. Raymond-Letron at the Département des Sciences Biologiques et Fonctionnelles/Laboratoire d'Histopathologie/UPS/INP/ENVT/US006 (Toulouse, France); and the staff at the animal facility of UMS US006/CREFRE (Toulouse, France). English proofreading was performed by Scientific Scripts (http://scientificscripts.com).

Address correspondence to: Fabienne Meggetto, UMR1037 INSERM/Université Toulouse III-Paul Sabatier, ERL5294 CNRS, 2 Avenue Hubert Curien, Oncopole Toulouse, Entrée C, CS 53717, 31037 Toulouse CEDEX 1, France. Phone: 33.5.62.74.45.39; E-mail: fabienne.meggetto@inserm.fr.

1. Lamant L, et al. Prognostic impact of morphologic and phenotypic features of childhood ALK-positive anaplastic large-cell lymphoma: results of the ALCL99 study. *J Clin Oncol*. 2011;29(35):4669–4676.
2. Savage KJ, et al. ALK- anaplastic large-cell lymphoma is clinically and immunophenotypically different from both ALK+ ALCL and peripheral T cell lymphoma, not otherwise specified: report from the International Peripheral T cell Lymphoma Project. *Blood*. 2008;111(12):5496–5504.
3. Hallberg B, Palmer RH. Mechanistic insight into ALK receptor tyrosine kinase in human cancer biology. *Nat Rev Cancer*. 2013;13(10):685–700.
4. Ferreri AJ, Govi S, Pileri SA, Savage KJ. Anaplastic large cell lymphoma, ALK-negative. *Crit Rev Oncol Hematol*. 2013;85(2):206–215.
5. Lai R, Ingham RJ. The pathobiology of the oncogenic tyrosine kinase NPM-ALK: a brief update. *Ther Adv Hematol*. 2013;4(2):119–131.
6. Jacobsen E. Anaplastic large-cell lymphoma, T-/null-cell type. *Oncologist*. 2006;11(7):831–840.
7. Kruczynski A, Delsol G, Laurent C, Brousset P, Lamant L. Anaplastic lymphoma kinase as a therapeutic target. *Expert Opin Ther Targets*. 2012;16(11):1127–1138.
8. Camidge DR, Doebele RC. Treating ALK-positive lung cancer — early successes and future challenges. *Nat Rev Clin Oncol*. 2012;9(5):268–277.
9. Christensen JG, et al. Cytoreductive antitumor activity of PF-2341066, a novel inhibitor of anaplastic lymphoma kinase and c-Met, in experimental models of anaplastic large-cell lymphoma. *Mol Cancer Ther*. 2007;6(12 pt 1):3314–3322.
10. Mologni L. Inhibitors of the anaplastic lymphoma kinase. *Expert Opin Investig Drugs*. 2012;21(7):985–994.
11. Gambacorti Passerini C, et al. Crizotinib in advanced, chemoresistant anaplastic lymphoma kinase-positive lymphoma patients. *J Natl Cancer Inst*. 2014;106(2):djt378.
12. Sahu A, Prabhash K, Noronha V, Joshi A, Desai S. Crizotinib: a comprehensive review. *South Asian J Cancer*. 2013;2(2):91–97.
13. Katayama R, et al. Therapeutic strategies to overcome crizotinib resistance in non-small cell lung cancers harboring the fusion oncogene EML4-ALK. *Proc Natl Acad Sci U S A*. 2011;108(18):7535–7540.
14. Han C, Yu Z, Duan Z, Kan Q. Role of microRNA-1 in human cancer and its therapeutic potentials. *Biomed Res Int*. 2014;2014:428371.
15. Han L, Witmer PD, Casey E, Valle D, Sukumar S. DNA methylation regulates MicroRNA expression. *Cancer Biol Ther*. 2007;6(8):1284–1288.
16. Han Y, et al. Restoration of shp1 expression by 5-AZA-2′-deoxycytidine is associated with downregulation of JAK3/STAT3 signaling in ALK-positive anaplastic large cell lymphoma. *Leukemia*. 2006;20(9):1602–1609.
17. Hayes J, Peruzzi PP, Lawler S. MicroRNAs in cancer: biomarkers, functions and 655 therapy. *Trends Mol Med*. 2014;20(8):460–469.
18. Lopez-Serra P, Esteller M. DNA methylation-associated silencing of tumor-suppressor microRNAs in cancer. *Oncogene*. 2012;31(13):1609–1622.
19. Baer C, Claus R, Plass C. Genome-wide epigenetic regulation of miRNAs in cancer. *Cancer Res*. 2013;73(2):473–477.
20. Fabbri M, Calin GA. Epigenetics and miRNAs in human cancer. *Adv Genet*. 2010;70:87–99.
21. Subramaniam D, Thombre R, Dhar A, Anant S. DNA methyltransferases: a novel target for prevention and therapy. *Front Oncol*. 2014;4:80.
22. Karahoca M, Momparler RL. Pharmacokinetic and pharmacodynamic analysis of 5-aza-2′-deoxycytidine (decitabine) in the design of its dose-schedule for cancer therapy. *Clin Epigenetics*. 2013;5(1):3.
23. Suzuki H, Maruyama R, Yamamoto E, Kai M. DNA methylation and microRNA dysregulation in cancer. *Mol Oncol*. 2012;6(6):567–578.
24. Henry JC, Azevedo-Pouly AC, Schmittgen TD. MicroRNA replacement therapy for cancer. *Pharm Res*. 2011;28(12):3030–3042.
25. Rebucci M, Michiels C. Molecular aspects of cancer cell resistance to chemotherapy. *Biochem Pharmacol*. 2013;85(9):1219–1226.
26. Ma J, Dong C, Ji C. MicroRNA and drug resistance. *Cancer Gene Ther*. 2010;17(8):523–531.
27. Zheng T, Wang J, Chen X, Liu L. Role of microRNA in anticancer drug resistance. *Int J Cancer*. 2010;126(1):2–10.
28. Merkel O, et al. Identification of differential and functionally active miRNAs in both anaplastic lymphoma kinase (ALK)+ and ALK- anaplastic large-cell lymphoma. *Proc Natl Acad Sci U S A*. 2010;107(37):16228–16233.
29. Desjobert C, et al. MiR-29a down-regulation in ALK-positive anaplastic large cell lymphomas contributes to apoptosis blockade through MCL-1 overexpression. *Blood*. 2011;117(24):6627–6637.
30. Matsuyama H, et al. miR-135b mediates NPM-ALK-driven oncogenicity and renders IL-17-producing immunophenotype to anaplastic large cell lymphoma. *Blood*. 2011;118(26):6881–6892.
31. Dejean E, et al. Hypoxia-microRNA-16 downregulation induces VEGF expression in anaplastic lymphoma kinase (ALK)-positive anaplastic large-cell lymphomas. *Leukemia*. 2011;25(12):1882–1890.
32. Bissels U, Bosio A, Wagner W. MicroRNAs are shaping the hematopoietic landscape. *Haematologica*. 2012;97(2):160–167.
33. Tili E, Michaille JJ, Costinean S, Croce CM. MicroRNAs, the immune system and rheumatic disease. *Nat Clin Pract Rheumatol*. 2008;4(10):534–541.
34. Monticelli S, et al. MicroRNA profiling of the murine hematopoietic system. *Genome Biol*. 2005;6(8):R71.
35. Undi RB, Kandi R, Gutti RK. MicroRNAs as haematopoiesis regulators. *Adv Hematol*. 2013;2013:695754.
36. Watanabe A, et al. The role of microRNA-150 as a tumor suppressor in malignant lymphoma. *Leukemia*. 2011;25(8):1324–1334.
37. Ito M, et al. MicroRNA-150 inhibits tumor invasion and metastasis by targeting the chemokine receptor CCR6, in advanced cutaneous T cell lymphoma. *Blood*. 2014;123(10):1499–1511.
38. Mishra A, Garzon R. The (miR)e of CTCL. *Blood*. 2014;123(10):1438.
39. He Y, Jiang X, Chen J. The role of miR-150 in normal and malignant hematopoiesis. *Oncogene*. 2014;33(30):3887–3893.
40. Honda N, et al. miR-150 down-regulation contributes to the constitutive type I collagen overexpression in scleroderma dermal fibroblasts via the induction of integrin β3. *Am J Pathol*. 2013;182(1):206–216.
41. Hassler MR, et al. Antineoplastic activity of the DNA methyltransferase inhibitor 5-aza-2′-deoxycytidine in anaplastic large cell lymphoma. *Biochimie*. 2012;94(11):2297–2307.
42. Kasprzycka M, Marzec M, Liu X, Zhang Q, Wasik MA. Nucleophosmin/anaplastic lymphoma kinase (NPM/ALK) oncoprotein induces the T regulatory cell phenotype by activating STAT3. *Proc Natl Acad Sci U S A*. 2006;103(26):9964–9969.
43. Levy DE, Inghirami G. STAT3: a multifaceted oncogene. *Proc Natl Acad Sci U S A*. 2006;103(27):10151–10152.
44. Zhang Q, et al. Multilevel dysregulation of STAT3 activation in anaplastic lymphoma kinase-positive T/null-cell lymphoma. *J Immunol*. 2002;168(1):466–474.
45. Dawson MA, Kouzarides T. Cancer epigenetics: from mechanism to therapy. *Cell*. 2012;150(1):12–27.
46. Wang LQ, Liang R, Chim CS. Methylation of tumor suppressor microRNAs: lessons from lymphoid malignancies. *Expert Rev Mol Diagn*. 2012;12(7):755–765.
47. Maia BM, Rocha RM, Calin GA. Clinical significance

of the interaction between non-coding RNAs and the epigenetics machinery: challenges and opportunities in oncology. *Epigenetics*. 2014;9(1):75–80.
48. Ambrogio C, et al. NPM-ALK oncogenic tyrosine kinase controls T cell identity by transcriptional regulation and epigenetic silencing in lymphoma cells. *Cancer Res*. 2009;69(22):8611–8619.
49. Piazza R, et al. Epigenetic silencing of the proapoptotic gene BIM in anaplastic large cell lymphoma through an MeCP2/SIN3a deacetylating complex. *Neoplasia*. 2013;15(5):511–522.
50. Zhang Q, Wang HY, Liu XB, Wasik MA. STAT5A is epigenetically silenced by the tyrosine kinase NPM1-ALK and acts as a tumor suppressor by reciprocally inhibiting NPM1-ALK expression. *Nat Med*. 2007;13(11):1341–1348.
51. Zhang Q, Wang HY, Marzec M, Raghunath PN, Nagasawa T, Wasik MA. STAT3- and DNA methyltransferase 1-mediated epigenetic silencing of SHP-1 tyrosine phosphatase tumor suppressor gene in malignant T lymphocytes. *Proc Natl Acad Sci U S A*. 2005;102(19):6948–6953.
52. Goffin J, Eisenhauer E. DNA methyltransferase inhibitors-state of the art. *Ann Oncol*. 2002;13(11):1699–1716.
53. Boumber Y, Issa JP. Epigenetics in cancer: what's the future? *Oncology (Williston Park)*. 2011;25(3):220–226.
54. Edlin R, et al. Azacitidine for the treatment of myelodysplastic syndrome, chronic myelomonocytic leukaemia and acute myeloid leukaemia. *Health Technol Asses*. 2010;14(suppl 1):69–74.
55. Curran MP. Decitabine: a review of its use in older patients with acute myeloid leukaemia. *Drug Aging*. 2013;30(6):447–458.
56. Daskalakis M, Blagitko-Dorfs N, Hackanson B. Decitabine. *Recent Results Cancer Res*. 2010;184:131–157.
57. Vijayaraghavalu S, Labhasetwar V. Efficacy of decitabine-loaded nanogels in overcoming cancer drug resistance is mediated via sustained DNA methyltransferase 1 (DNMT1) depletion. *Cancer Lett*. 2013;331(1):122–129.
58. Bezman NA, Chakraborty T, Bender T, Lanier LL. miR-150 regulates the development of NK and iNKT cells. *J Exp Med*. 2011;208(13):2717–2731.
59. Chen S, et al. Re-expression of microRNA-150 induces EBV-positive Burkitt lymphoma differentiation by modulating c-Myb in vitro. *Cancer Sci*. 2013;104(7):826–834.
60. Zhou Y, Ness SA. Myb proteins: angels and demons in normal and transformed cells. *Front Biosci (Landmark Ed)*. 2011;16:1109–1131.
61. Cogswell JP, et al. Mechanism of c-Myc regulation by c-Myb in different cell lineages. *Mol Cell Biol*. 1993;13(5):2858–2869.
62. Zhang J, Luo N, Luo Y, Peng ZP, Zhang T, Li SL. microRNA-150 inhibits human CD133-positive liver cancer stem cells through negative regulation of the transcription factor c-Myb. *Int J Oncol*. 2012;40(3):747–756.
63. Fawal M, et al. A "liaison dangereuse" between AUF1/hnRNPD and the oncogenic tyrosine kinase NPM-ALK. *Blood*. 2006;108(8):2780–2788.
64. Gouble A, Grazide S, Meggetto F, Mercier P, Delsol G, Morello D. A new player in oncogenesis: AUF1/hnRNPD overexpression leads to tumorigenesis in transgenic mice. *Cancer Res*. 2002;62(5):1489–1495.
65. Jiang X, et al. Blockade of miR-150 maturation by MLL-fusion/MYC/LIN-28 is required for MLL-associated leukemia. *Blood*. 2012;120(4):524–535.
66. Brenner C, et al. Myc represses transcription through recruitment of DNA methyltransferase corepressor. *EMBO J*. 2005;24(2):336–346.
67. Mutze K, et al. DNA methyltransferase 1 as a predictive biomarker and potential therapeutic target for chemotherapy in gastric cancer. *Eur J Cancer*. 2011;47(12):1817–1825.
68. Foyil KV, Bartlett NL. Brentuximab vedotin and crizotinib in anaplastic large-cell lymphoma. *Cancer J*. 2012;18(5):450–456.
69. Voena C, Chiarle R. The battle against ALK resistance: successes and setbacks. *Expert Opin Investig Drugs*. 2012;21(12):1751–1754.
70. Mosse YP, et al. Safety and activity of crizotinib for paediatric patients with refractory solid tumours or anaplastic large-cell lymphoma: a Children's Oncology Group phase 1 consortium study. *Lancet Oncol*. 2013;14(6):472–480.
71. Zdzalik D, et al. Activating mutations in ALK kinase domain confer resistance to structurally unrelated ALK inhibitors in NPM-ALK-positive anaplastic large-cell lymphoma. *J Cancer Res Clin Oncol*. 2014;140(4):589–598.
72. Mummaneni P, Shord SS. Epigenetics and oncology. *Pharmacotherapy*. 2014;34(5):495–505.
73. Ceccon M, Mologni L, Bisson W, Scapozza L, Gambacorti-Passerini C. Crizotinib-resistant NPM-ALK mutants confer differential sensitivity to unrelated Alk inhibitors. *Mol Cancer Res*. 2013;11(2):122–132.
74. Gorre ME, et al. Clinical resistance to STI-571 cancer therapy caused by BCR-ABL gene mutation or amplification. *Science*. 2001;293(5531):876–880.
75. Kobayashi S, et al. EGFR mutation and resistance of non-small-cell lung cancer to gefitinib. *N Engl J Med*. 2005;352(8):786–792.
76. La Rosee P, et al. In vitro efficacy of combined treatment depends on the underlying mechanism of resistance in imatinib-resistant Bcr-Abl-positive cell lines. *Blood*. 2004;103(1):208–215.
77. Chen Y, et al. Oncogenic mutations of ALK kinase in neuroblastoma. *Nature*. 2008;455(7215):971–974.
78. Janoueix-Lerosey I, et al. Somatic and germline activating mutations of the ALK kinase receptor in neuroblastoma. *Nature*. 2008;455(7215):967–970.
79. George RE, et al. Activating mutations in ALK provide a therapeutic target in neuroblastoma. *Nature*. 2008;455(7215):975–978.
80. Mosse YP, et al. Identification of ALK as a major familial neuroblastoma predisposition gene. *Nature*. 2008;455(7215):930–935.
81. Liu C, et al. MicroRNA expression profiling identifies molecular signatures associated with anaplastic large cell lymphoma. *Blood*. 2013;122(12):2083–2092.